Auger recombination of excitons in one-dimensional systems

Feng Wang,[1,3] Yang Wu,[1,3] Mark S. Hybertsen,[2,3] and Tony F. Heinz[1,3]
[1]*Departments of Physics and Electrical Engineering, Columbia University, New York, New York 10027, USA*
[2]*Department of Applied Physics and Applied Mathematics, Columbia University, New York, New York 10027, USA*
[3]*Center for Electron Transport in Molecular Nanostructures, Columbia University, New York, New York 10027, USA*
(Received 24 December 2005; revised manuscript received 25 March 2006; published 20 June 2006)

In tightly confined one-dimensional (1D) systems, the effective Coulomb interaction is greatly enhanced and optical transitions generally lead to the formation of strongly bound excitons. When more than one exciton is present, the Coulomb interaction also leads to rapid exciton-exciton annihilation through an Auger recombination process. This effect, which may be significant even at low exciton densities, can be described by a rate law governing two-body interactions. The Auger recombination rate for excitons in a strongly confined 1D system is analyzed. The rate increases sharply with exciton binding energy, but varies only weakly with temperature. An explicit expression for the Auger recombination rate in terms of the exciton binding energy, optical matrix element and reduced carrier mass is derived for a two-band model in which the Coulomb interaction is approximated by a point-contact potential. Results for the prototypical 1D system of single-walled carbon nanotubes are obtained and compared with experiment.

DOI: 10.1103/PhysRevB.73.245424 PACS number(s): 73.22.Lp, 73.43.Cd, 78.67.−n, 79.20.Fv

I. INTRODUCTION

Strongly quantum-confined one-dimensional (1D) materials exhibit many distinctive electrical and optical properties. In these systems, a single quantized transverse electron and hole subband dominates. One important driving force for these diverse physical phenomena is the dramatically enhanced Coulomb interaction arising both from the spatial confinement of the carriers and from the reduced charge-screening effects that are present in these 1D systems. The enhanced Coulomb interaction in 1D semiconductors leads to the formation of tightly bound exciton states when electron-hole pairs are excited, as well as to an increased role for interactions involving multiple charge carriers. Auger recombination, also known in this context as exciton-exciton annihilation, involves such multiple-carrier interactions. In this process electron-hole pairs undergo nonradiative recombination, with the released energy transferred directly to other charge carriers.

Auger recombination is known to be significant for bulk and two-dimensional semiconductors at high carrier densities.[1–4] In view of the enhanced electron-electron interactions,[5–9] one would expect Auger processes to assume still greater prominence in 1D structures, just as it dominates the multicarrier dynamics in zero-dimensional (0D) semiconductor nanoparticles.[10] Rapid Auger recombination of excitons has indeed been observed in the prototypical 1D structure of single-wall carbon nanotubes (SWNTs).[11–13] This interaction is sufficiently strong that it dominates nanotube carrier dynamics when multiple excitations are present in SWNTs,[11–13] and a recombination rate orders of magnitude higher than that characteristic of bulk materials has been measured.[11] Similar effects have also been reported for semiconductor nanorods.[14] The strength of the Auger recombination process appears to be an intrinsic feature of tightly confined 1D materials. In view of the fundamental interest in understanding this multicarrier process and its implications for a range of applications of 1D materials, there is a strong motivation to develop a theoretical understanding of what controls the behavior and rate of this process.

The present work aims to fill this need by examining the Auger process for strongly confined 1D systems. The strongly confined isolated 1D structure under consideration here is different from previously investigated weakly confined structures such as epitaxially grown semiconductor quantum wires.[15–17] These wires typically have widths of tens to hundreds of nanometers and are embedded in high-dielectric constant material. In such systems, multiple subbands (especially for the holes in the valence bands) contribute. Furthermore, the enhancement of Coulomb interaction is slight, and exciton binding energies remain below or comparable to thermal energy at room temperature. Consequently, electron-hole pairs can be described simply as free carriers, and the Auger process in these materials is similar to that of bulk media. In particular, the Auger recombination process exhibits an activated behavior as a function of the carrier temperature, unless phonon assisted processes play an important role.[15] The existence of an energy barrier is a direct result of the need to conserve both energy and momentum in the Auger process, together with the free electron and hole dispersion relations. This behavior is different for strongly 1D materials with large exciton binding energies. Because the exciton states already contain components corresponding to electron and hole wave functions with large momenta, there is no energy barrier for the Auger recombination process. Consequently, the Auger rate exhibits little temperature dependence and can be large even at relatively low temperatures.

We consider neutral systems that have been excited with N excitons. The Auger recombination process of tightly bound excitons in 1D structures can be described by an exciton annihilation rate of $\Gamma_{\text{Auger}}=(A/L)\cdot N\cdot(N-1)$, where A is the Auger constant, and L the length of the nanostructure. To determine the rate constant A in terms of the underlying Coulomb interaction, we make use of a simplified point-contact model of the carrier-carrier interaction. Assuming

single parabolic bands for the electron and hole, we are able to derive explicit expressions for the Auger recombination rate A. Further, within the context of the model, the strength of the carrier-carrier interaction can be calibrated from the exciton binding energy, a quantity frequently amenable to experimental measurement. In this way, we characterize the interplay between exciton binding and Auger recombination for strongly 1D materials. As a specific example, we apply the analysis to Auger recombination in SWNTs. For SWNTs of 1-nm diameter, the experimental exciton binding of ~300 meV (Ref. 18) implies a room-temperature Auger constant of $A \sim 0.6$ ps^{-1} μm. This remarkably rapid rate compares well with the value obtained recently from direct experimental measurements of the ultrafast dynamics of photoexcited SWNTs.[11]

II. MODEL OF THE 1D SYSTEM AND ITS CARRIER INTERACTIONS

We first describe the relevant electronic states in our model. We consider the Auger recombination of excitons in an idealized one-dimensional system. We assume that the electrons and holes can be described by a two-band model with an allowed optical transition. Higher subbands are assumed to be separated by an energy larger than the exciton binding energy allowing them to be neglected. Each band (electron and hole) is further assumed to be parabolic and is treated using an envelope function approximation (effective mass approximation). The single-particle excitations of the system are carriers in the conduction and valence bands. We write a free electron of momentum $\hbar k_e$ as $|k_e\rangle = e^{ik_e r}|u_{c,k_e}\rangle$, where $|u\rangle$ is the periodic part of the Bloch wave function. Correspondingly, we denote a hole of momentum $\hbar k_h$ as $|k_h\rangle$, which represents a missing valence electron in state $e^{-ik_h r}|u_{v,-k_h}\rangle$. We assume parabolic dispersion relations of $\varepsilon_{c,k_e} = E_g + \frac{\hbar^2 k_e^2}{2m_e}$ and $\varepsilon_{v,k_h} = -\frac{\hbar^2 k_h^2}{2m_h}$ for the conduction and valence bands, respectively. Here E_g is the energy of the (direct) band gap, and m_e and m_h are, respectively, electron and hole effective masses.

Within the effective mass approximation, we can introduce the Coulomb interaction for an electron-hole pair through a Hamilton,

$$H = H_e + H_h + V_{e\text{-}h} = -\frac{\hbar^2 \nabla_R^2}{2m_{ex}} - \frac{\hbar^2 \nabla_r^2}{2\mu} + V(r). \tag{1}$$

The right-hand side of the equation is expressed in terms of the relative electron-hole position $r = r_e - r_h$ and the electron-hole center-of-mass position $R = (m_e r_e + m_h r_h)/(m_e + m_h)$. The corresponding expressions for the electron and hole kinetic energies (for the bands described above) involve the exciton mass $m_{ex} = m_e + m_h$ and the reduced mass $\mu = m_e m_h/(m_e + m_h)$. Provided that the characteristic length scale for the bound exciton is greater than the physical diameter of the 1D system and encompasses ten or more atomic spacings, the envelope function approximation should be reasonable. In the example discussed below, this will be the case. In our model, the electron-hole interaction term $V(r)$ is treated as a point-contact interaction, $V(r) = -U\delta(r)$, with (an attractive) strength parameter U. This both regularizes the Coulomb interaction for 1D and simplifies the analysis. For the relatively strong exciton binding under discussion here, this model captures the main effects. For clarity, we neglect electron spin in our initial discussion, but consider its effect below after having derived the pertinent relations.

Electron-hole pairs in the presence of the contact interaction can form excitons. The electron and hole in the exciton have relative momenta $\hbar q \equiv \frac{m_h k_e - m_e k_h}{(m_e + m_h)}$ that extend up to a value on the order of $\hbar\kappa \equiv \mu U/\hbar$, determined by the strength of the Coulomb interaction. The spatial extent of the exciton wave function is consequently on the order of $1/\kappa = \hbar^2/(\mu U)$. The exciton binding energy is $E_b = \frac{\hbar^2\kappa^2}{2\mu}$, and the total energy for an exciton of momentum $\hbar K$ is given by $E_K = E_g - E_b + \frac{\hbar^2 K^2}{2m_{ex}}$. The envelope function for the exciton in the internal coordinate is $\psi(r) = \sqrt{\kappa/2}\exp(-\kappa|r|)$. For the Auger calculation, the corresponding wave functions for the exciton states can be written explicitly in terms of electron-hole pair states $|k_e;k_h\rangle = |k_e\rangle|k_h\rangle$ as

$$|K\rangle = \sum_{k_e,k_h} \psi^K_{k_e,k_h}|k_e;k_h\rangle = \sum_{k_e,k_h} \delta_{K,k_e+k_h}\sqrt{\frac{1}{\kappa L}}\frac{2\kappa^2}{\kappa^2+q^2}|k_e;k_h\rangle. \tag{2}$$

In calculating the rate of the Auger process, we consider an initial state comprised of two excitons with center of mass momenta $\hbar K$ and $\hbar P$ described by the wave function

$$|i\rangle = |K\rangle|P\rangle = \left(\sum_{k_e',k_h'} \psi^K_{k_e',k_h'}|k_e';k_h'\rangle\right) \times \left(\sum_{k_e'',k_h''} \psi^P_{k_e'',k_h''}|k_e'';k_h''\rangle\right), \tag{3}$$

where the ground-state exciton wave function $\psi^K_{k_e,k_h}$ is as defined in Eq. (2). The final state consists of an ionized electron of momentum $\hbar k_e$ and an ionized hole of momentum $\hbar k_h$, described by $\langle f| = \langle k_e, k_h|$. In our discussion, we neglect the influence of the Coulomb interaction on the final states. This approximation is justified by the fact that the final state of the electron or hole will have excess energy comparable to the band gap, so that the Coulomb potential leads to a relatively small correction.

III. CALCULATION OF THE AUGER RECOMBINATION RATE OF EXCITONS

Following the general approach previously introduced in Ref. 19 for Auger recombination of tightly bound excitons in three dimensions, we calculate the exciton Auger recombination rate for our 1D problem by perturbation theory using the initial and final states described above. The possible underlying scattering processes are summarized in Fig. 1 with explicit reference to the *electron* transitions in the valence as well as conduction band. In process A, the Coulomb interaction between the electrons in the excitons results in an interband scattering event where one of the holes in the valence band is filled and the other electron is excited higher into the

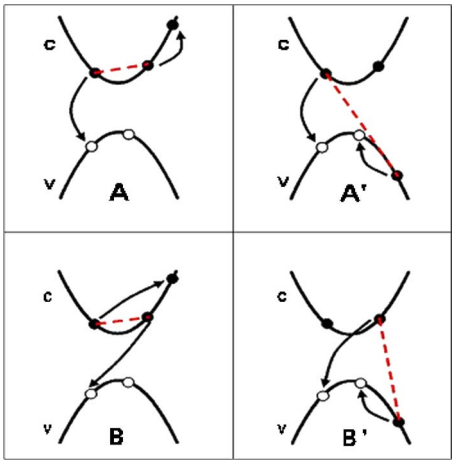

FIG. 1. (Color online) Illustration of scattering processes leading to Auger recombination for two electron-hole pairs. The dotted line describes a pair of electrons that scatter by their Coulomb interaction. The arrows indicate the final state of the electrons after scattering in the Auger process. Processes A and B correspond to scattering of two electrons in the conduction band, while processes A' and B' involve scattering of an electron in the conduction band with an electron in the valence band.

conduction band. The process A' involves Coulomb scattering between one of the excited electrons in the conduction band with one of the electrons in the filled states of the valence band such that both holes in the valence band are filled, but an excited hole is left behind deeper in the valence band. The B (B') process is just the electron (hole) exchange counterpart of the A (A') process. The calculation follows the procedure introduced for excitons in bulk materials in Ref. 19. The different allowed processes are described by topologically distinct Feynman diagrams shown in Fig. 2. This allows a crisp distinction between the initial exciton states that are left out of Fig. 1. The first class of diagrams, A and A', can be seen to represent electron-hole annihilation within one exciton, while the second class, B and B', describes an electron (hole) recombining with the hole (electron) of the

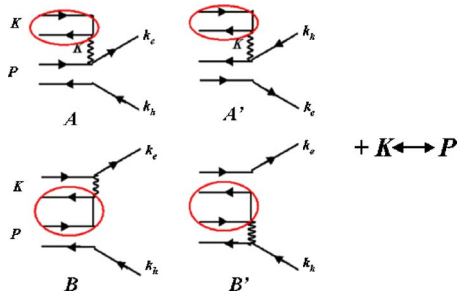

FIG. 2. (Color online) Feynman diagrams for the Auger recombination process. The solid lines with forward- (backward-) going arrows denote electrons (holes), and the wavy lines represent the Coulomb interaction. Time progresses from left to right. The initial state consists of two excitons with momenta of K and P; the final state consists of a free electron with momentum k_e and a hole with momentum k_h. The exchange of momenta K and P leads to the other four diagrams that are not shown explicitly, but are included in the calculation.

other exciton involved in the Auger process. In addition, we must retain the diagrams in which the initial exciton states are exchanged. For this initial discussion, the spin degree of freedom is ignored.

It is straightforward to show that the Feynman diagrams generate matrix elements

$$M_A + M_{A'} = \sum_{k_e',k_h'} \psi^K_{k_e',k_h'} \cdot V_K \langle u_{v,-k_h'} | u_{c,k_e'} \rangle \cdot \delta_{k_e+k_h,K+P} \times [\psi^P_{k_e-K,k_h} \langle u_{c,k_e} | u_{c,k_e-K} \rangle - \psi^P_{k_e,k_h-K} \langle u_{v,-k_h} | u_{v,-k_h+K} \rangle],$$

$$M_B + M_{B'} = - \sum_{k_e',k_h'} \delta_{k_e+k_h,K+P} \times [V_{k_e-k_e'} \psi^K_{k_e',k_h'} \psi^P_{k_e-K,k_h} \cdot \langle u_{v,-k_h'} | u_{c,k_e-K} \rangle \times \langle u_{c,k_e} | u_{c,k_e'} \rangle - V_{k_h-k_h'} \psi^P_{k_e',k_h'} \times \psi^K_{k_e,k_h-P} \cdot \langle u_{v,-k_h+P} | u_{c,k_e'} \rangle \langle u_{v,-k_h} | u_{v,-k_h'} \rangle], \quad (4)$$

where V_q is the Fourier transform of the electron-electron interaction and represents the potential for a momentum transfer of q. We have neglected the umklapp processes in our derivation, which can be shown to be small following the argument of Ref. 19 for the bulk calculation. The relative sign between the A and B diagrams follows from their exchange relationship. The relative sign between the primed and unprimed diagrams can be thought of intuitively as the difference between effective electron-electron and electron-hole interactions. These expressions are generally applicable to exciton-exciton interactions, independent of dimensionality.

The overlap integrals can be evaluated using $k \cdot p$ perturbation theory.[20] According to this analysis, the periodic part of the conduction and valence band for our model can be expressed as

$$|u_{c,k}\rangle = |u_{c,k_0}\rangle + \frac{\hbar}{m_0} \frac{\langle u_{v,k_0} | (k-k_0) \cdot p | u_{c,k_0} \rangle}{\varepsilon_{c,k_0} - \varepsilon_{v,k_0}} |u_{v,k_0}\rangle, \quad (5)$$

$$|u_{v,k}\rangle = |u_{v,k_0}\rangle + \frac{\hbar}{m_0} \frac{\langle u_{c,k_0} | (k-k_0) \cdot p | u_{v,k_0} \rangle}{\varepsilon_{v,k_0} - \varepsilon_{c,k_0}} |u_{c,k_0}\rangle, \quad (6)$$

where ε_{c,k_0} and ε_{v,k_0} are the energies of the conduction and valence band at wave vector k_0 and m_0 is the free-electron mass. It is apparent from the above equations that for two electron states with relatively small momentum difference ($k-k' \ll G_0$, where G_0 is the reciprocal-lattice vector), the overlap integral $\langle u_{c,k_e} | u_{c,k_e'} \rangle \approx 1$. The overlap integral between the conduction band and valence band assumes the form

$$\langle u_{v,-k_h}|u_{c,k_e}\rangle = \frac{\hbar}{m_0}\frac{\langle u_{v,-k_h}|(k_e+k_h)\cdot p|u_{c,-k_h}\rangle}{\varepsilon_{c,-k_h}-\varepsilon_{v,-k_h}} \approx \frac{\hbar(k_e+k_h)}{m_0}\frac{\langle p\rangle_{vc}}{E_g}. \quad (7)$$

Here we assume that $\varepsilon_{c,-k_h}-\varepsilon_{v,-k_h}\approx E_g$ and that $\langle u_{v,-k_h}|p|u_{c,-k_h}\rangle \approx \langle u_{v,0}|p|u_{c,0}\rangle \equiv \langle p\rangle_{vc}$. These approximations are valid for k_e, $k_h \ll G_0$, corresponding to charge carriers near the band edge and consistent with the approximate evaluation of the final rate below.

Specializing to the case of 1D systems and using the point-interaction potential $V(r)=U\cdot\delta(r)$ expressed in momentum space as $V_q=U/L$, we obtain

$$M_A + M_{A'} \approx \frac{U}{L}\cdot\sqrt{\kappa L}\cdot\frac{\hbar K}{m_0 E_g}\langle p\rangle_{vc}\delta_{k_e+k_h,K+P} \times[\psi^P_{k_e-K,k_h}-\psi^P_{k_e,k_h-K}], \quad (8)$$

$$M_B + M_{B'} \approx -2\frac{U}{L}\cdot\sqrt{\kappa L}\cdot\frac{\hbar k_e}{m_0 E_g}\langle p\rangle_{vc}\delta_{k_e+k_h,0}\cdot\psi^0_{k_e,k_h}. \quad (9)$$

Comparing the matrix elements of processes A, A' with B, B', we note that the ratio of the former to the latter differs by a factor including K/k_e. Because the initial momentum K is determined by thermal energy, which is much smaller than other energy scales, the processes A,A', make a comparatively small contribution to Auger recombination of tightly bound excitons in 1D systems. The weakness of processes A and A' can be understood intuitively as a consequence of the fact that the Coulomb potential from the electron and hole of the second excitons largely cancel each other out when acting on the first exciton. This is not the case when the annihilated electron and hole are in different excitons. We have thus for the overall matrix element

$$M = M_A + M_{A'} + M_B + M_{B'} + (K\leftrightarrow P) \approx M_B + M_{B'} + (K\leftrightarrow P) = -4\frac{U}{L}\cdot\sqrt{\kappa L}\cdot\frac{\hbar k_e}{m_0 E_g}\langle p\rangle_{vc}\delta_{k_e+k_h,0}\cdot\psi^0_{k_e,k_h}. \quad (10)$$

We can now calculate the decay rate $\Gamma_{K,P}$ for the Auger recombination of two excitons with momenta K and P using Fermi's golden rule,

$$\Gamma_{K,P} = \frac{2\pi}{\hbar}\sum_{k_e,k_h}|M|^2(1-n_{c,k_e})(1-n_{v,k_h})\cdot\delta(E_K+E_P-\varepsilon_{c,k_e}-\varepsilon_{v,k_h}) \approx \frac{32}{k_{e0}L}\cdot\frac{\hbar\kappa^2}{\mu}\left(\frac{\hbar k_{e0}}{m_0 E_g}\langle p\rangle_{vc}\right)^2\left(\frac{2\kappa^2}{\kappa^2+k_{e0}^2}\right)^2. \quad (11)$$

To obtain the second expression, the population factors $(1-n_{c,k_e})$ and $(1-n_{v,k_h})$ for available scattering states for an electron in the conduction band and a hole in the valence band are taken as 1, since thermal populations at these states are negligible. We also recognize that the energy scale of the band gap is typically much larger than that of thermal excitations. Conservation of energy and momentum then leads to a final electron wave vector $k_{e0}=\sqrt{2\mu(E_g-2E_b)}/\hbar$. Note that at this level of approximation, the Auger rate does not depend on the values of the exciton momenta K and P and consequently the Auger rate has no dependence on temperature for a thermalized ensemble of excitons.

We can eliminate κ in favor of the exciton binding energy E_b. For convenience, we further simplify the expression by expanding in terms of $E_b/2E_g$ to obtain

$$\Gamma_{K,P} \approx 512\cdot\omega_{vc}\frac{1}{k_{e0}L}\cdot\left(\frac{\mu}{m_0}\right)\left(\frac{E_b}{E_g}\right)^3. \quad (12)$$

Here we have introduced a phenomenological rate parameter related to the interband transition strength, $\omega_{vc}\equiv\langle p\rangle_{vc}^2/\hbar m_0$. For allowed transitions in typical materials, $\hbar\omega_{vc}$ will have a value in the order of 1 eV.

In the analysis so far, we have neglected electron spin, as well as the multiband nature of real materials. The spin state of the excitons in the sample will depend on the experimental conditions. In the circumstances of Ref. 11, a simple and likely scenario for the initial state is that both excitons are singlets, but there is no correlation between them. In this case, the estimated Auger rate will be halved—half of the time the electron in one exciton will have the wrong spin relative to the hole in the other exciton and the electron-hole annihilation in processes B and B' will be forbidden. The multiband nature of carbon nanotube makes possible a new process where electrons and holes are being excited to second bands. Estimation of this rate is beyond the scope of the present work.

For N excitations in a 1D structure of length L, the overall Auger recombination rate can be found by considering the rate of binary collisions. It assumes the form

$$\Gamma_{\text{Auger}} = \frac{A}{L}\cdot N(N-1) \approx A\cdot L\cdot n^2, \quad (13)$$

where A is the Auger constant and n the line density of excitons in the limit of large exciton population. Using Eq. (12), applicable to $N=2$, and inserting another factor of 1/2 arising from spin considerations for singlet excitons, we obtain the expression for the Auger constant

$$A = 128\frac{\omega_{vc}}{k_{e0}}\cdot\left(\frac{\mu}{m_0}\right)\left(\frac{E_b}{E_g}\right)^3. \quad (14)$$

This final expression highlights the intimate relationship between the strength of the exciton binding energy and the rate of the Auger recombination process. Physically, one expects this behavior. Strong excitonic binding supplies the quantum mechanical coupling to the relatively high momenta of the final electron and hole states required in the recombination process. As in the earlier expression, within the approximations of this analysis, the Auger rate does not dependent on the temperature of the excitons.

IV. DISCUSSION AND APPLICATION OF ANALYSIS TO CARBON NANOTUBES

As a specific example, we apply our result to an attractive physical realization of a strongly confined 1D system, single-

walled carbon nanotubes (SWNTs). The electronic states in SWNTs have quantized angular momentum, with each quantum number corresponding to a different van Hove subband. For nanotubes of 1-nm diameter, all the subbands are well separated and the coupling between the subbands due to the Coulomb interaction is believed to be small.[6] As such, we can consider electrons and holes of only the lowest conduction and valence band and treat the Coulomb potential as effectively one-dimensional. It has also been shown that even for nanotubes of diameter less than 0.8 nm, the excitons have a characteristic spatial extent of ~ 1.2 nm,[8,18] almost 10 times the lattice constant and comparable to that of bulk ZnSe and ZnTe.[21] The envelope function approach for the excitons and the two-band effective mass model for the single-particle states thus are reasonable.

The exciton binding energy is known experimentally[18] to be $E_b = \frac{\hbar^2\kappa^2}{2\mu} \approx 300$ meV, while the band-gap energy is $E_g \approx 1.3$ eV. The effective electron and hole masses are $m_e \approx m_h \approx 0.1 m_0$ and the momentum matrix element $\langle p \rangle_{vc} \approx 0.8\hbar(1/\text{Å})$ can be estimated within the tight-binding model.[22] With these parameters, we obtain a predicted Auger constant of $A = 0.6$ ps^{-1} μm. This corresponds to an Auger recombination lifetime of 1.7 ps for two excitons in 1-μm long nanotube.

Considering the significant simplifications in the model, the predicted two-exciton Auger recombination lifetime is in good agreement with the measured[11] value of 3 ps for 1-μm long nanotube. This agreement underscores the importance of enhanced electron-hole interaction and excitonic effects in 1D structures such as nanotubes, a feature intrinsic to our model. In comparison, the calculated rate based on uncorrelated electron-hole pair as initial states is orders of magnitudes lower.

In summary, we have calculated the Auger recombination rate for excitons in neutral, strongly confined 1D nanostructures. We found that the Auger recombination rate rapidly increases with binding energy of the exciton, a general result for strongly confined 1D nanostructures. Furthermore, there is no energy barrier for this Auger process and, hence, no strong dependence on temperature, in marked contrast to the behavior for free charge carriers. In the experimentally interesting case of SWNTs, the nonradiative Auger recombination channel can be expected to dominate the carrier dynamics once multiple excitations are present. This situation is relevant for many possible photonic applications. For instance, the Auger process will limit the sustainable carrier densities in SWNTs, rendering population inversion difficult to achieve. On the other hand, the extremely rapid Auger relaxation suggests SWNTs application in ultrafast optics, such as a saturable absorber for femtosecond lasers.[23]

ACKNOWLEDGMENTS

We would like to thank Louis Brus and Gordana Dukovic for helpful discussions. This work was supported primarily by the Nanoscale Science and Engineering Initiative of the National Science Foundation under NSF Grants No. CHE-0117752 and No. ECS-05-07111; and by the New York State Office of Science, Technology, and Academic Research (NYSTAR).

[1] A. Sugimura, Appl. Phys. Lett. **39**, 21 (1981).
[2] G. P. Agrawal and N. K. Dutta, *Long-Wavelength Semiconductor Lasers* (Van Nostrand Reinhold Company, New York, 1986).
[3] D. J. Roulston, *Bipolar Semiconductor Devices* (McGraw-Hill, New York, 1990).
[4] M. A. Green, *Silicon Solar Cells: Advanced Principles and Practice* (UNSW Press, Sydney, 1995).
[5] T. Ando, J. Phys. Soc. Jpn. **66**, 1066 (1997).
[6] V. Perebeinos, J. Tersoff, and P. Avouris, Phys. Rev. Lett. **92**, 257402 (2004).
[7] C. L. Kane and E. J. Mele, Phys. Rev. Lett. **93**, 197402 (2004).
[8] C. D. Spataru, S. Ismail-Beigi, L. X. Benedict, and S. G. Louie, Phys. Rev. Lett. **92**, 077402 (2004).
[9] H. Zhao and S. Mazumdar, Phys. Rev. Lett. **93**, 157402 (2004).
[10] V. I. Klimov, A. A. Mikhailovsky, D. W. McBranch, C. A. Leatherdale, and M. G. Bawendi, Science **287**, 1011 (2000).
[11] F. Wang, G. Dukovic, E. Knoesel, L. E. Brus, and T. F. Heinz, Phys. Rev. B **70**, 241403(R) (2004).
[12] Y. Z. Ma, J. Stenger, J. Zimmermann, S. M. Bachilo, R. E. Smalley, R. B. Weisman, and G. R. Fleming, J. Chem. Phys. **120**, 3368 (2004).
[13] Y. Z. Ma, L. Valkunas, S. L. Dexheimer, S. M. Bachilo, and G. R. Fleming, Phys. Rev. Lett. **94**, 157402 (2005).
[14] H. Htoon, J. A. Hollingsworth, R. Dickerson, and V. I. Klimov, Phys. Rev. Lett. **91**, 227401 (2003).
[15] M. Takeshima, Phys. Rev. B **31**, 992 (1985).
[16] R. A. Abram, R. W. Kelsall, and R. I. Taylor, J. Phys. Chem. Solids **49**, 607 (1988).
[17] J. Wang and J. P. Leburton, IEEE Photonics Technol. Lett. **6**, 1091 (1994).
[18] F. Wang, G. Dukovic, L. E. Brus, and T. F. Heinz, Science **308**, 838 (2005); G. Dukovic, F. Wang, D. Song, M. Y. Sfeir, T. F. Heinz, and L. E. Brus, Nano Lett. **5**, 2314 (2005).
[19] G. M. Kavoulakis and G. Baym, Phys. Rev. B **54**, 16625 (1996).
[20] E. O. Kane, in *Semiconductors and Semimetals*, edited by R. K. Willardson and A. C. Beer (Academic, New York, 1966), Vol. 1, p. 75.
[21] P. Y. Yu and M. Cardona, *Fundamentals of Semiconductors* (Springer, Berlin, 2001).
[22] R. Saito, G. Dresselhaus, and M. S. Dresselhaus, *Physical Properties of Carbon Nanotubes* (Imperial College Press, London, 1998).
[23] S. Y. Set, H. Yaguchi, Y. Tanaka, and M. Jablonski, J. Lightwave Technol. **22**, 51 (2004).